PROCEEDINGS OF SCIENCE

Recent progresses on the γ-ray observations of DAMPE

Zhao-Qiang Shen,[a,*] **Kai-Kai Duan,**[a] **Wei Jiang,**[a] **Zun-Lei Xu**[a,b] **and Xiang Li**[a,b] **for the DAMPE collaboration**

[a] *Key Laboratory of Dark Matter and Space Astronomy, Purple Mountain Observatory, Chinese Academy of Sciences, Nanjing, China*

[b] *School of Astronomy and Space Science, University of Science and Technology of China, Hefei, China*

E-mail: zqshen@pmo.ac.cn

The DArk Matter Particle Explorer (DAMPE) is a space-borne high-energy particle detector launched on 17 December 2015. It can observe the γ-ray sky from $\sim$ 2 GeV to 10 TeV with the acceptance at most 1800 cm^2 sr. With over 7.5 years of continuous operation, DAMPE has surveyed the whole sky for about 15 times and collected more than 300,000 candidate photon events. In the last few years, the understanding of the payload has been improved and the instrumental response functions have been calibrated with the on-board data. Besides, progresses have been made on the γ-ray line search, point source detection, diffuse emission analysis, and transient source monitoring. In the talk and this accompanying proceeding, the latest results on these topics are reported.

38th International Cosmic Ray Conference (ICRC2023)
26 July – 3 August, 2023
Nagoya, Japan

*Speaker

PoS(ICRC2023)670

1. Introduction

The DArk Matter Particle Explorer (DAMPE) is a cosmic-ray detector and a pair-converting γ-ray telescope covering a wide energy range from GeV to $\sim$ 10 TeV [1, 2]. As shown in the Fig. 1, from top to bottom, DAMPE consists of a Plastic Scintillator strip Detector (PSD), a Silicon-Tungsten tracKer-converter (STK), a BGO imaging calorimeter (BGO) and a NeUtron Detector (NUD). The PSD measures the particle charge and acts as an anti-coincidence detector. The STK converts the incident γ rays to electron pairs and records the subsequent trajectories. The BGO measures the energies of incident particles and images the profiles of showers. The NUD further enhances the electron/proton separation capacity.

DAMPE was launched on 17 December 2015 and is now operating in a 500-km solar synchronous orbit with an inclination of $\sim 97^\circ$ and an period of around 95 min [2, 3]. Since the launch, the spacecraft has been working in the *sky-survey* mode [2], in which the boresight of the telescope is pointing towards the geocentric zenith. Because of the orbit and the observation mode, DAMPE surveys the full sky twice every year.

At the present, with over 7.5 years of continuous operation, DAMPE has performed the full-sky surveys for about 15 times and collected more than 300,000 candidate photon events above 2 GeV. We have not only performed some calibrations with the flight data but also made some progresses on the γ-ray astronomy. I will first present the calibrations relevant for photons in Sec. 2, and then introduce the γ-ray astronomy achieved since the previous ICRCs [4, 5] in Sec. 3.

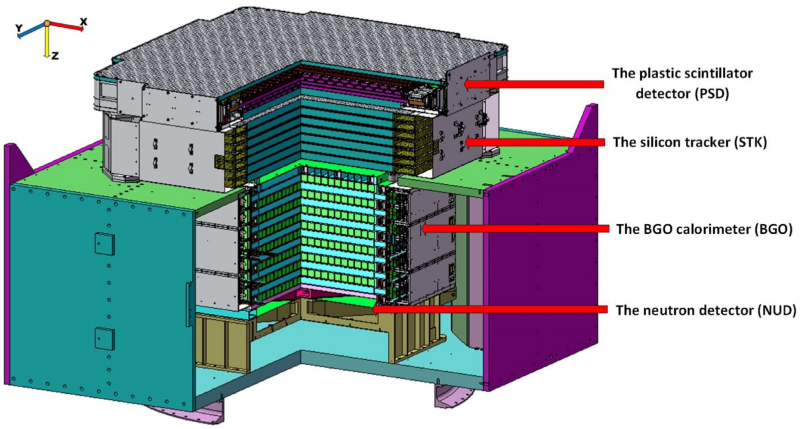

Figure 1: The schematic view of the DAMPE detector [2].

2. Calibration, photon data and instrumental response functions (IRFs)

On-orbit calibrations on each sub-detector have been carried out since the launch [3]. Recently, a global alignment of all the sub-detectors is performed [6]. The STK self-alignment is first conduct by minimizing the displacement between the hit positions and trajectory impact points. The PSD and BGO are then aligned based on the tracks aligned for the STK. After applying this correction, the flight data better match the Monte Carlo (MC) simulation, and both the angular resolution and the energy resolution of the γ-ray data are improved (see Fig. 9-10 in [6]).

A highly efficient selection algorithm is applied to distinguish γ-ray photons from the charged cosmic rays (CRs) [7]. In brief, the electromagnetic/hadronic separation is firstly performed based on the morphology of the shower deposit in the calorimeter; then the conversion track in the STK is reconstructed and selected; finally the charge particle rejections are made with the PSD. After the procedure, the fraction of charged CRs in the events drops to $\lesssim 1\%$ over 10 GeV. Recently, the rejection threshold of the PSD is further improved and the STK is also adopted to assist the anti-coincidence. With this update, the contaminations from the protons and electrons decrease by $\lesssim 50\%$ and $\lesssim 15\%$ respectively at the cost of merely $\lesssim 3\%$ γ-ray acceptance.

The boresight alignment corrects for the angular deviation between the DAMPE payload and the satellite system. Following the procedure in [8], an updated boresight alignment is performed with the 7-yr photons around the Vela pulsar. The rotation angles along the x, y and z axes to align these two coordinate systems are $(\psi, \theta, \phi) = (0.103°, 0.038°, -0.130°) \pm (0.012°, 0.011°, 0.016°)$. These Euler angles are consistent with the previous results in 1σ uncertainties, suggesting no significant time-dependent variation.

With the improved instrumental calibrations and data selection algorithm, the DAMPE `v6.0.3` photon data are produced. There are 302,952 candidate γ-ray events with energy larger than 2 GeV observed by DAMPE from 1 January 2016 to 31 December 2022. The data up to 31 December 2021 between 3 GeV and 1 TeV will be publicly available in late July this year.[1] The photon data are classified into two event types according to the triggers they satisfy: those fulfill the High Energy Trigger pattern are HET events (`evtype=1`), and those otherwise are LET events (`evtype=0`) [9].

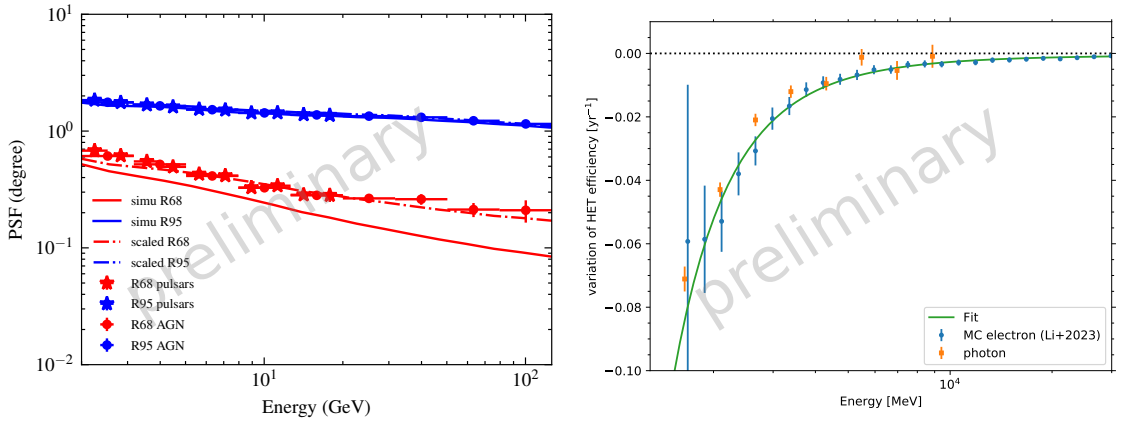

Figure 2: The calibration of IRFs with flight data. The left panel shows 68% and 95% containment radii of the MC (solid line) and calibrated (dot-dashed) PSF. The right panel shows the variation of HET efficiency. The blue and orange points represent the variation of MC electrons and observed photons.

The IRFs are the parameterized representations of the instrumental responses to incident photons, which depends on the γ-ray selection algorithm. They are factorized into three components: the effective area, the point-spread function (PSF) and the energy dispersion function, and are derived from the MC simulation [9]. IRFs are critical for the data analysis, and thereby should match the actual response. The PSF and effective area have also been calibrated with the flight data recently and the corrections are incorporated into the up-to-date version of `DmpST`.

[1]The data and the analysis software `DmpST` are available in https://dampe.nssdc.ac.cn.

PSF describes the distribution of angular deviation between the true and reconstructed incident directions. In [10], 7.2-yr photons from pulsars (Vela, Geminga and Crab) and active galaxy nuclei (AGNs) are adopted to derive the containment radii of the PSF. As shown in the left panel of Fig. 2, the 68% containment radii (the points) are slightly larger than the MC ones shown in the solid lines. An energy-dependent factor is multiplied to the extension of the PSF core component $\sigma_{\rm core}$ to compensate for the difference. The factor is derived by fitting the measured containment radii, and the results after the correction are shown in dot-dashed lines.

Due to the on-orbit pre-scale of Low Energy Trigger [2, 11], the majority of DAMPE photons are HET events. In [12], the High Energy Trigger threshold in energy is found to increase gradually with time, which is mainly caused by the irradiation damage of BGO bars. To quantify the efficiency variation of HET photons, the observed photons are binned into several energy bins, the change of counts observed per year is evaluated, which is shown with orange points in the right panel of Fig. 2. The result is consistent with the energy-dependent HET trigger efficiency variation of MC electrons. The one-side LogParabola function is adopted to fit the relation. The exposure map is

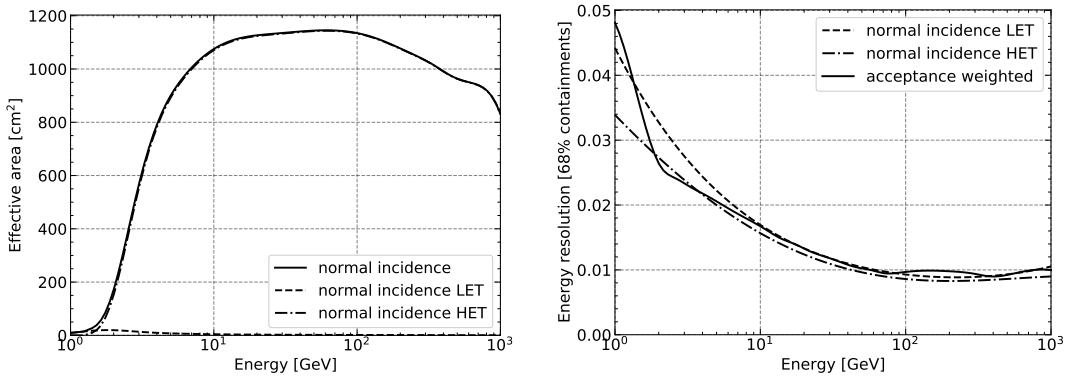

Figure 3: The γ-ray performance of DAMPE. From the left to right are the total effective area and energy resolution. The HET efficiency correction is not applied to the effective area. The containment radii of the calibrated PSF are shown in the left panel of Fig. 2.

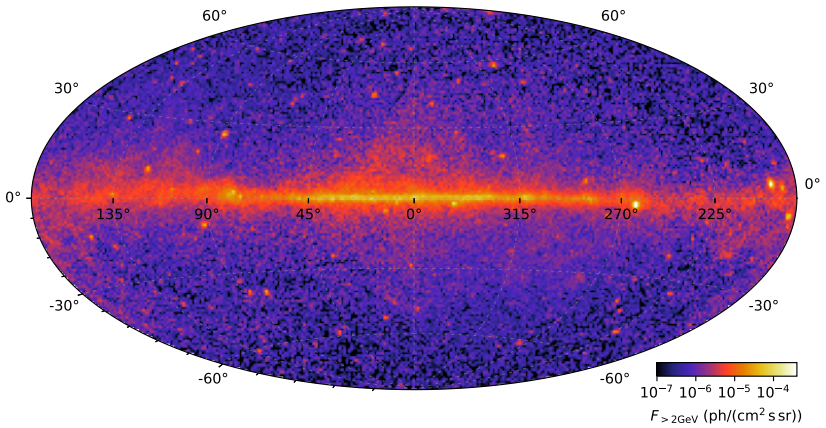

Figure 4: The map of the integrated flux above 2 GeV derived with 7.2-yr DAMPE LET and HET photons. The time variation of HET efficiency is considered in the calculation of the exposure map.

corrected by taking the efficiency change into account.

The DAMPE γ-ray performance with the latest calibration and data selection is presented in Fig. 3. With the calibrated IRFs, the map of the integrated flux above 2 GeV can be calculated and is shown in Fig. 4. Lots of structures and point sources are visible in the map, and some of them are analyzed as presented in Sec. 3.

3. γ-ray astronomy with DAMPE

3.1 γ-ray spectral lines

Dark matter (DM) particles may annihilate or decay and create γ-ray lines [13, 14]. Since the distinct spectral features are hard to be produced in known astrophysical processes, a robust detection would be a smoking-gun signature of DM. Thanks to the thick BGO calorimeter with 32 radiation length, DAMPE has the highest energy resolution in the GeV−TeV range (see the right panel of Fig. 3). Benefited from the advantage, DAMPE can effectively search for γ-ray lines with a good sensitivity and a small systematic uncertainty.

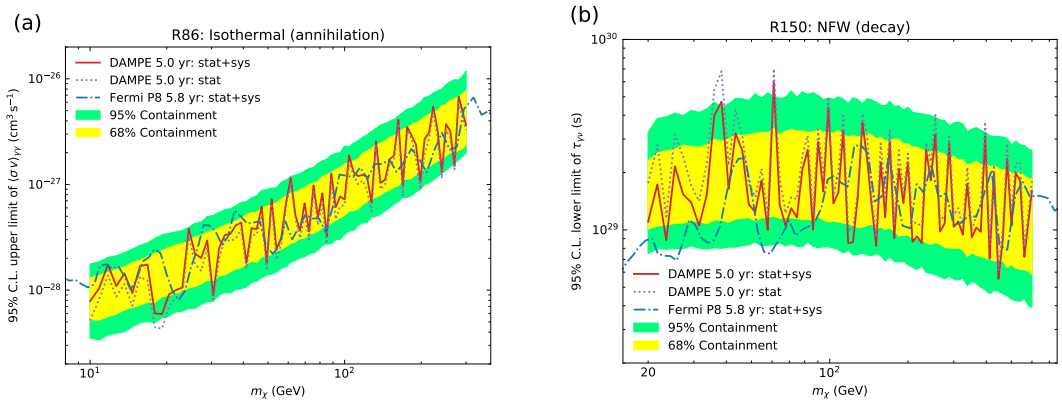

Figure 5: The constraints on DM parameter space derived from the γ-ray line search with DAMPE [15]. The left panel shows the 95% upper limits on the DM annihilation cross section for isothermal DM distribution. The right panel shows the 95% lower limits on the DM decay lifetime.

In [15], a systematic search of the spectral lines produced in the Galaxy was performed. To further improve the sensitivity, two dedicated data sets are developed [16]: the *LineSearch* data set that balances the energy resolution with the acceptance, and the *BgoOnly* data set which contains the events converted in the calorimeter. Lines are searched for in the signal-to-noise optimized regions of interests (ROIs) assuming various DM density profiles. No lines with significance larger than 3σ are found, so the DM constraints with systematic uncertainties are presented, some of which are shown in Fig. 5. Although DAMPE has an acceptance smaller by a factor of $\sim$ 10 than *Fermi*-LAT, similar constraints on the DM parameters are achieved and below the DM mass of 100 GeV the decay lifetime are even stronger by a factor of a few.

3.2 Point sources and transient sources

γ rays are the most energetic form of the electromagnetic radiation. It plays an important role in unveiling the most violent processes of the sources. γ-ray point sources were first identified by

SAS-2 in 1970s. Now over 6658 sources have been detected by *Fermi*-LAT [17].

In [10], a DAMPE point source catalog is built with 7.2 years of observation. Using the blind search method based on the Li-Ma formula [18], 248 point sources are detected with TS values larger than 25 and their locations are shown in Fig. 6. After associating the sources with the *Fermi*-LAT 4FGL-DR3 catalog [17], the type of each source is found. As shown in the statistic in Tab. 1, the majority of the detected point sources are AGNs. More details can be found in [10].

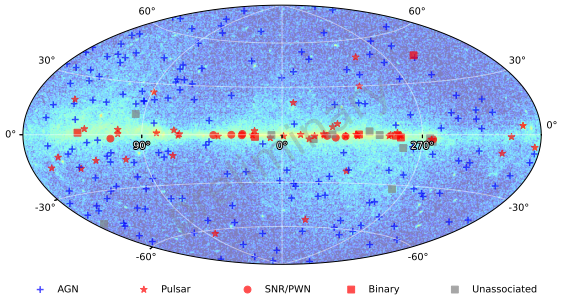

Figure 6: The significant point sources (TS ≥ 25) detected in 7.2-yr DAMPE data. The markers present the types of the associated sources.

Source Type	Number
AGN	175
Pulsar	46
SNR/PWN	10
Binary	6
Unassociated	11
Total	248

Table 1: The number of each source type.

DAMPE also pays close attention to the transient sources. Some of the bright AGN flares are reported: TXS 0646−176, BL Lac, PKS 0903−57, PKS 1830−211, S4 1800+44, 3C 279 and CTA 102 [19]. DAMPE also detected the photon events associated with the brightest γ-ray burst GRB 221009A [20].

3.3 Galactic center excess (GCE)

GCE is a $10^\circ - 15^\circ$ spherical excess in the Galaxy center (GC) with the spectrum peaked at ∼ 2 GeV [21, 22]. It is robust against various systematic uncertainties [23–26]. It can be explained with the DM annihilation [21] or a population of millisecond pulsars [27].

In [28], the GCE is searched for with 7.2-yr DAMPE LET and HET photon data. It is detected with 7.9σ significance between 2 GeV and 31.6 GeV. The spatial distribution is fitted with the DM annihilation distribution of the generalized NFW profile $\rho_{\rm nfw}(r) = \rho_0/[(r/r_{\rm s})^{\gamma}(1+r/r_{\rm s})^{3-\gamma}]$ and the optimal inner slope is $\gamma = 1.16 \pm 0.10$, which is consistent with that of the *Fermi*-LAT [29]. If the excess is explained with the DM annihilation into $b\bar{b}$, DM particles with mass $m_\chi = 45 \pm 11$ GeV and cross section $\langle\sigma v\rangle = (2.2 \pm 0.3) \times 10^{-26}$ cm^3 s^{-1} is required. The DM parameter space is also consistent with the *Fermi*-LAT [24, 26]. More results can be found in the poster of [28] and the upcoming paper.

3.4 Fermi bubbles (FBs)

FBs consist of two large bubbles, each of which is approximately 40° wide and extends to 55° above and below the GC [30, 31]. They may be originated from the AGN [30, 32] or the wind [33, 34] in the GC.

In [35], 4.8-yr DAMPE data are adopted to search for the emission from the FBs. The analyses are updated with 6.0 years of DAMPE data. The FBs are detected with a significance of $\sim 17.8\sigma$. In the fitting without the FBs template, there is a residual emission that matches the morphology

of FBs. A 3.7σ curvature in spectrum is found. If fitted with the PowerLawExpCutoff, the index is $\gamma_1 = 1.8 \pm 0.1$ and the cutoff energy is $E_{\rm cut} = 102 \pm 41$ GeV. The spectra of the north and south lobes are analyzed separately and are found to match with each other. Generally speaking, the spectrum of FBs is well consistent with the *Fermi*-LAT [31]. The emission from the cocoon is also searched for and it is only weakly detected with a significance of $\sim 3.3\sigma$.

4. Summary

DAMPE has been stably operating for about 7.5 years and has collected more than 300,000 candidate photon events above 2 GeV. Calibrations on the simulations and IRFs are performed with flight data. Researches are also done with DAMPE photon data: γ-ray lines in the Galaxy are searched for, point source catalog is constructed, GCE and FBs are analyzed and significantly detected.

Acknowledgments

The DAMPE mission is funded by the strategic priority science and technology projects in space science of Chinese Academy of Sciences. In China the data analysis is supported in part by the National Key Research and Development Program of China (No. 2022YFF0503301), the National Natural Science Foundation of China (Nos. 12003074, 12173098, 12220101003, 11921003, 11903084, 12003076 and 12022503), the Scientific Instrument Developing Project of the Chinese Academy of Sciences (No. GJJSTD20210009), the CAS Project for Young Scientists in Basic Research (No. YSBR061), the Young Elite Scientists Sponsorship Program by CAST (No. YESS20220197), the 100 Talents Program of Chinese Academy of Sciences, Youth Innovation Promotion Association CAS, and the Entrepreneurship and Innovation Program of Jiangsu Province. In Europe the activities and the data analysis are supported by the Swiss National Science Foundation (SNSF), Switzerland, the National Institute for Nuclear Physics (INFN), Italy, and the European Research Council (ERC) under the European Union's Horizon 2020 research and innovation programme (No. 851103).

References

[1] J. Chang. *Chin. J. Spac. Sci.* **34** (2014) 550.

[2] DAMPE collaboration. *Astropart. Phys.* **95** (2017) 6 [1706.08453].

[3] DAMPE collaboration. *Astropart. Phys.* **106** (2019) 18 [1907.02173].

[4] S.-J. Lei, Q. Yuan, Z.-L. Xu et al. in proceedings of *ICRC2017*, PoS(ICRC2017)616 (2017).

[5] X. Li, K.-K. Duan, W. Jiang et al. in proceedings of *ICRC2019*, PoS(ICRC2019)576 (2019).

[6] Y.-X. Cui, P.-X. Ma, G.-W. Yuan et al. *Nucl. Inst. Methods A* **1046** (2023) 167670 [2209.09440].

[7] Z.-L. Xu, K.-K. Duan, Z.-Q. Shen et al. *Res. Astron. Astrophys.* **18** (2018) 027 [1712.02939].

[8] W. Jiang, X. Li, K.-K. Duan et al. *Res. Astron. Astrophys.* **20** (2020) 092 [2001.01804].

[9] K.-K. Duan, W. Jiang, Y.-F. Liang et al. *Res. Astron. Astrophys.* **19** (2019) 132 [1904.13098].

[10] K.-K. Duan, Z.-L. Xu, Z.-Q. Shen et al. in proceedings of *ICRC2023*, PoS(ICRC2023)670 (2023).

[11] Y.-Q. Zhang, J.-H. Guo, Y. Liu et al. *Res. Astron. Astrophys.* **19** (2019) 123.

[12] W.-H. Li, C. Yue, Y.-Q. Zhang et al. *to be submitted* (2023).

[13] L. Bergström and H. Snellman. *Phys. Rev. D* **37** (1988) 3737.

[14] A. Ibarra and D. Tran. *Phys. Rev. Lett.* **100** (2008) 061301 [0709.4593].

[15] DAMPE collaboration. *Sci. Bull.* **67** (2022) 679 [2112.08860].

[16] Z.-L. Xu, K.-K. Duan, W. Jiang et al. *Front. Phys.* **17** (2022) 34501 [2107.13208].

[17] Fermi-LAT collaboration. *Astrophys. J. Suppl. Ser.* **260** (2022) 53 [2201.11184].

[18] T.P. Li and Y.Q. Ma. *Astrophys. J.* **272** (1983) 317.

[19] Z.-L. Xu et al. *ATel* **14993** (2021); Z.-L. Xu et al. *ATel* **14621** (2021); K.-K. Duan et al. *ATel* **13643** (2020); Z.-L. Xu et al. *ATel* **12705** (2019); Z.-L. Xu et al. *ATel* **12562** (2019); Z.-L. Xu et al. *ATel* **11246** (2018); Z.-L. Xu et al. *ATel* **9901** (2016).

[20] K.-K. Duan, Z.-L. Xu, Z.-Q. Shen et al. *GCN CIRCULAR* **32973** (2022).

[21] L. Goodenough and D. Hooper. arXiv:0910.2998 (2009).

[22] F. Calore, I. Cholis, C. McCabe and C. Weniger. *Phys. Rev. D* **91** (2015) 063003 [1411.4647].

[23] B. Zhou, Y.-F. Liang, X. Huang et al. *Phys. Rev. D* **91** (2015) 123010 [1406.6948].

[24] F. Calore, I. Cholis and C. Weniger. *J. Cosmol. Astropart. Phys.* **2015** (2015) 038 [1409.0042].

[25] M. Ackermann, M. Ajello, A. Albert et al. *Astrophys. J.* **840** (2017) 43 [1704.03910].

[26] I. Cholis, Y.-M. Zhong, S.D. McDermott et al. *Phys. Rev. D* **105** (2022) 103023 [2112.09706].

[27] K.N. Abazajian. *J. Cosmol. Astropart. Phys.* **2011** (2011) 010 [1011.4275].

[28] Z.-Q. Shen, K.-K. Duan, Z.-L. Xu el al. in proceedings of *ICRC2023*, PoS(ICRC2023)671 (2023).

[29] T. Daylan, D.P. Finkbeiner, D. Hooper et al. *Phys. Dark Univ.* **12** (2016) 1 [1402.6703].

[30] M. Su, T.R. Slatyer and D.P. Finkbeiner. *Astrophys. J.* **724** (2010) 1044 [1005.5480].

[31] Fermi-LAT collaboration. *Astrophys. J.* **793** (2014) 64 [1407.7905].

[32] F. Guo and W.G. Mathews. *Astrophys. J.* **756** (2012) 181 [1103.0055].

[33] R.M. Crocker and F. Aharonian. *Phys. Rev. Lett.* **106** (2011) 101102 [1008.2658].

[34] G. Mou, F. Yuan, D. Bu et al. *Astrophys. J.* **790** (2014) 109 [1403.2129].

[35] Z.-Q. Shen, K.-K. Duan, Z.-L. Xu et al. in proceedings of *ICRC2021*, PoS(ICRC2021)640 (2021).